Am J Cancer Res 2023;13(10):4931-4943
www.ajcr.us /ISSN:2156-6976/ajcr0153045

Original Article

IL25$^+$ macrophages are a key determinant of treatment resistance of IL17RB$^+$ breast cancer

Yukinori Ozaki[1,2,3], Keiichi Kinowaki[4], Hidetaka Kawabata[5], Chie Kudo-Saito[1]

[1]Department of Immune Medicine, National Cancer Center Research Institute, Tokyo 104-0045, Japan; [2]Department of Medical Oncology, Toranomon Hospital, Tokyo 105-8470, Japan; [3]Breast Oncology Center, Cancer Institute Hospital of Japanese Foundation for Cancer Research, Tokyo 135-8550, Japan; [4]Department of Pathology, Toranomon Hospital, Tokyo 105-8470, Japan; [5]Department of Breast and Endocrine Surgery, Toranomon Hospital, Tokyo 105-8470, Japan

Received August 20, 2023; Accepted October 3, 2023; Epub October 15, 2023; Published October 30, 2023

Abstract: Recurrence and metastasis are resistant to multimodal treatments, and are the major causes of death in breast cancer. Accumulating evidence suggests that the IL17RB signaling pathway plays a key role in progression and metastasis of breast cancer. Clinical significance of the IL17RB positivity in tumor tissues has been also reported as a poor prognostic factor in breast cancer. However, the molecular mechanisms underlying the poor prognosis of patients with IL17RB$^+$ breast cancer, particularly the immunological aspects, remain to be fully elucidated, and elimination of the IL17RB$^+$ tumors has not been practically achieved in clinical settings. In this study, we identified a distinct molecular mechanism underlying the intractability of the IL17RB$^+$ tumors through tumor biological and immunological investigation using mouse and human breast cancer cells transduced with *il17rb* gene. IL17RB overexpression in tumor cells confers cancer stemness, including high invasive and self-renewal abilities, and high resistance to CDK4/6 inhibitors that have been considered as a promising agent for treating breast cancer despite the limited efficacy. In the mice implanted with the IL17RB$^+$ tumors, IL25$^+$ macrophages (Møs) are expanded locally in tumor tissues and systemically in spleen, and promote the IL17RB$^+$ tumor progression directly by intensifying the tumor functions, and indirectly via impairment of anti-tumor effector CTLs and NK cells utilizing the secreted IL25. Blocking IL25 with the specific mAb, however, interferes the adverse events, and successfully elicits significant anti-tumor efficacy in combination with CDK4/6 inhibitors providing better survival in murine mammary tumor models. These results suggest that the IL25$^+$ Mø is a key determinant of building the solid treatment resistance of the IL17RB$^+$ breast cancer. Targeting the IL17RB-IL25 axis may be a promising strategy to improve clinical outcomes in the treatment of breast cancer patients, particularly with IL17RB$^+$ tumors.

Keywords: Breast cancer, IL17RB, IL25, macrophages, CDK4/6 inhibitors, cancer stem, immunosuppression, immune exhaustion, immune dysfunction

Introduction

Breast cancer is one of the most common cancers and the second largest cause of cancer-related deaths [1]. Many cases experience recurrence and metastasis resistant to multimodal treatments, including mastectomy, breast-conserving surgery, chemotherapy, hormone therapy, radiotherapy, molecular targeted therapy, and immunotherapy [2]. In the molecular targeted therapy, targeting cyclin-dependent kinases 4 and 6 (CDK4/6) has attracted great attention as a promising strategy for treating breast cancer because of a key driver of the cell cycle required for the initiation and progression of tumor cells. Many CDK4/6 inhibitors (CDKIs), including abemacicrib/LY-2835219 and palbociclib/PD0332991, have been clinically developed and approved for treating estrogen receptor$^+$HER2$^-$ advanced or metastatic breast cancer in combination with hormone/endocrine therapy [3]. However, the therapeutic efficacy is limited in the clinical settings. About 10% of patients show innate resistance, and most patients acquire resistance after several years as the first-line treatment, and after a short time as the second-line treatment. Recent studies have revealed the molec-

ular mechanisms underlying the CDKI resistance: For example, amplification and overexpression of the CDK4/6, activation of other mitogenic signaling pathways, and loss or mutation of RB1 [4, 5]. However, no breakthrough has been established for overcoming the CDKI resistance in clinical settings. As an alternative strategy to enhance the therapeutic efficacy, CDKI therapy has been combined with many other therapeutics, such as estrogen receptor antagonists, chemotherapeutics, inhibitors targeting the upstream receptor tyrosine kinases, such as HER2, EGFR, and FGFR, and inhibitors targeting other CDKs, such as CDK2 and CDK7, in numerous clinical trials [5, 6]. However, most trials have failed.

Accumulating evidence suggests that the signaling pathway of interleukin-17 receptor β (IL17RB) drives initiation, proliferation, invasion, survival, and anti-apoptosis of cancer stem-like tumor cells upon the binding to its ligands, IL17B or IL17E/IL25, in various types of cancer, including breast cancer [7, 8]. In clinical settings, high and frequent expression of the IL17RB in tumor tissues has been reported as a critical poor prognostic factor in breast cancer [7, 8]. These suggest that IL17RB should be targeted in the treatment of refractory breast cancer. However, elimination of the IL17RB$^+$ tumors has not been practically achieved in the clinical settings, and relationships between the tumoral IL17RB positivity and the CDKI responses remain unclear. Tumor cells are known to plastically evolve through interplay with the host environment, particularly immune network, and the reciprocal evolution further increases tumor heterogeneity leading to refractory cancer [9]. Therefore, better understanding and interference of the oncoimmunological interplay must be important for eradication of IL17RB$^+$ refractory breast cancer.

In this study, we validated the clinical significance of the IL17RB positivity in breast cancer by own immunohistochemical analysis of patient-derived tumor tissues, and then attempted to elucidate the molecular mechanisms underlying the poor prognosis of patients with IL17RB$^+$ breast cancer through tumor biological and immunological investigation using mouse and human IL17RB-transduced breast cancer cells. We also evaluated in vivo anti-tumor efficacy induced by agents targeting the key molecule in the mechanisms in combination with CDKIs toward clinical practice.

Materials and methods

Clinical analysis

For immunohistochemical analysis for IL17RB expression, tumor tissues were surgically resected from stage I-III breast cancer patients receiving no neo-adjuvant chemotherapy at Toranomon Hospital (September 2006-December 2013), according to the protocol (No. 845 and No. 1327) approved by the Institutional Review Board of the Toranomon Hospital (n = 115). Informed consent was obtained from all individual participants included in the study. After deparaffinization, formalin-fixed and paraffin-embedded tumor tissue sections were stained with HRP-conjugated anti-IL17RB mAb (Clone 938923; Novus) or the isotype control, and were treated with DAB and hematoxylin for visualization. Two pathological researchers microscopically observed the molecular expressions, and classified the IL17RB expression patterns into 3 groups according to the intensity: Level 0, no expression; Level 1, weak expression; and Level 2, strong expression. Relationships between the expression levels and the clinicopathological data were statistically analyzed. All activities were conducted in accordance with the ethical principles of the Declaration of Helsinki.

Mice and cell lines

Five-week-old female BALB/c mice and BALB/c-nu nude mice were purchased from Charles River Laboratories in Japan, and were maintained under pathogen-free conditions. Mice were used according to the protocol (No. T17-055) approved by the Animal Care and Use Committee at the National Cancer Center Research Institute. Murine mammary cancer 4T1 cells and human breast cancer MCF7 cells were purchased from ATCC, and were tested for Mycoplasma negativity using a Hoechst-staining detection kit (MP Biomedicals). The cells were expanded and frozen in liquid nitrogen to avoid changes occurred by a long-term culture before experiments.

Establishment of IL17RB transfectants

For stable overexpression of IL17RB, IL17RB^{low} 4T1 cells and IL17RB$^-$ MCF7 cells were used,

since only 4T1 was available to us among murine breast cancer cell lines, and another human breast cancer cell line MDA-MB-231 available to us highly expressed IL17RB, although the two cell lines are known to have different phenotypes, 4T1 like triple-negative breast cancer versus MCF7 like Luminal A subtype. These cells were transfected with a plasmid vector pCMV6-ENTRY encoding murine *il17rb* (NM_019583; Origene) or human *il17rb* (NM_018725; Origene), or the empty vector as mock control using a polymerase-based transfection reagent jetPEI (Polyplus) according to the manufacturer's instructions. After limiting dilution, the transduction efficacy was evaluated by flow cytometry and immunostaining using anti-mouse IL17RB-PE (BioLegend), anti-human IL17RB-AF488 (R&D), or each isotype control, and several clones with IL17RB overexpression were chosen for assays. IL17RA expression was also analyzed by staining with anti-mouse IL17RA-FITC (Abcam). In the immunostaining, two cytospin slides per clone were stained with mAbs following fixation with 4% PFA, and the immunofluorescence intensity was automatically measured as pixel counts at 400× magnification (almost 50 cells per field × 3 fields per slide) using the LSM700 Laser Scanning Microscope (Carl Zeiss) as described before [10]. To show the spontaneous colony formation, tumor cells were cultured in a slide chamber (Ibidi) for 24 hours without staining.

Characterization of tumor cells

Tumor functions were assessed as described before [11, 12]: Cell proliferation (3 days) by counting the number of cells in the culture, self-renewability (3 days) by counting the number of sphere colonies (> ø 50 μm) using a 24-well Ultra-Low Attachment Surface plate (Coaster), and cell invasion (4 hours) by counting the number of cells passing through a matrigel-coated membrane of a transwell chamber (Corning). To assess sensitivity to CDK4/6 inhibitors, tumor cells (5 × 10^3 cells/well) were cultured with abemaciclib/LY2835219 (CDKI-LY; AdooQ) or palbociclib/PD0332991 (CDKI-PD; AdooQ) for 2 days, and the proliferation was measured by a colorimetric assay using WST1 solution (Takara). Graphs were depicted as the percentage of the control cultured with no agents (100%). In the in vivo setting, 4T1 cells (5 × 10^5) were subcutaneously (s.c.) implanted into BALB/c mice, and CDKIs (5 mg/kg) or PBS as a control were orally administered in the mice daily for 5 days (start on day 3-5 after tumor implantation). MCF7 cells (1 × 10^6) were s.c. implanted into immunodeficient nude mice, and the mice received the 2-cycle CDKI treatment (days 5-9, and days 16-20). Tumor volume (0.5 × Length × Width^2, mm^3) was measured every 2-3 days. One week after the last treatment, subcutaneous tumors and spleens were harvested from the mice, and the isolated cells were analyzed by flow cytometry. To assess cytotoxic activity of anti-tumor effector cells in the mice, spleen cells (SPCs) were pre-stimulated with the H-2L^d-restricted tumor antigen peptide AH1 (1 μg/ml; MBL) that is derived from the gp70 envelope protein expressed in 4T1 cells [13] for 6 days, and CD8$^+$ T cells were sorted as CTLs using a BD IMag system with magnetic particle-conjugated anti-CD8 mAb (BD Biosciences) according to the manufacturer's instructions. DX5$^+$ NK cells were similarly sorted from SPCs. These cells were cocultured with target tumor cells (4T1 or Yac1) at ET ratio = 20-50:1 for 4 hours, and the specific lysis of tumor cells was assessed using the Immunocyto Cytotoxicity Detection Kit (MBL) according to the manufacturer's instructions.

In vivo therapy

BALB/c mice were s.c. implanted with 4T1 cells (5 × 10^5), and received the following treatments: oral administration with CDKI-LY (5 mg/kg) or PBS as a control daily for 5 days (start on day 3-5 after tumor implantation), and/or i.p. injection with anti-IL25 blocking mAb (Clone 35B; BioLegend) or mouse IgG (mIgG, Clone MOPC-21; BioXCell) as a control at 10 mg/kg on twice a week. Nude mice were s.c. implanted with MCF7 cells (1 × 10^6), and received the following treatments: oral administration with CDKI-LY or PBS daily on days 5-9 and days 16-20, and/or i.p. injection with anti-IL25 mAb or mIgG on days 5, 9, 16 and 20. Tumor volume was measured, and mouse survival was observed in a setting.

Characterization of splenic macrophages

F4/80$^+$ cells were sorted from SPCs or tumor-infiltrating cells (TILs) as macrophages (Møs) using a BD IMag system (BD Biosciences) with biotin-conjugated anti-F4/80 mAb (BioLegend) and magnetic particle-conjugated streptavidin (BD Biosciences), and were tested for IL25

expression by immunostaining with anti-mouse IL25-PE (Invitrogen) after 2-hour-culture for cell attachment. After scraping, the Møs (1 × 10^6 cells/10 ml) were cultured for 6 days, and the supernatant fluids were tested for IL25 using an ELISA kit (Invitrogen). We mainly used splenic Møs for experiments, since the number of tumoral Møs was too small to conduct many different assays with a sufficient number of n per experiment for confirming the validity of the data. To assess the Mø effect on tumor cells, the Mø supernatants or recombinant IL25 (10 ng/ml; R&D) were added to tumor culture (1 × 10^5/well) in the presence of anti-IL25 mAb or mIgG (10 μg/ml), and 3 days later, the tumor functions were tested as described above. To assess the Mø effect on CTLs, Møs (2.5 × 10^6/well) were cocultured with the AH1-prestimulated CD8$^+$ T cells (1 × 10^6/well) in the presence of the AH1 peptide (10 μg/ml), IL2 (100 IU/ml), and anti-IL25 mAb or mIgG (10 μg/ml) for 6 days, and the sorted CD8$^+$ T cells were tested for cytotoxic activity as described above. In the in vivo setting, the Møs (3 × 10^5) were s.c. coinjected with tumor cells (3 × 10^5) in mice, and the subcutaneous tumors were directly injected with anti-IL25 mAb or mIgG (100 μg/tumor) to interfere the Mø-derived IL25 action in the tumor microenvironment on days 3 and 10 after coinjection.

Flow cytometric analysis

After Fc blocking, cells were stained with the following immunofluorescence-conjugated antibodies: anti-CD3e-BUV496 (BD), anti-CD4-BV785 (BioLegend), anti-CD8-BUV395 (BD), anti-CD45-PE-Cy7 (BioLegend), anti-DX5-APC-Cy7 (BioLegend), anti-PD1-BV510 (BioLegend), anti-TIM3-BV605 (BioLegend), anti-CD11b-BV-711 (BioLegend), anti-F4/80-BV510 (BioLegend), anti-mouse IL25-PE (Invitrogen), and the appropriate isotype control. For intracellular staining, cells were treated with Cytofix/Cytoperm solution (BD) before antibody staining. Data were acquired using a BD LSR Fortessa X-20 cytometer (BD), and were analyzed by FlowJo software (BD). Before defining the specific molecular expressions, debris was firstly excluded by FSC/SSC, and immunofluorescence intensity was compared to the isotype control.

Statistical analysis

Data are presented as means ± SDs unless otherwise specified. Experiments were repeated at least three times to confirm the reproducibility. Significant differences (P value < 0.05) were statistically evaluated using GraphPad Prism 7 software (MDF) or EZR software version 1.53. To compare between two groups, the data were analyzed by the unpaired two-tailed Student's t test. To compare multiple groups, the data were analyzed by one-way ANOVA, followed by the Bonferroni post-hoc test for pairwise comparison of groups on the basis of the normal distributions. Non-parametric groups were analyzed by the Mann-Whitney test. In the combination therapy, significance to the single treatment was evaluated using a two-way ANOVA with Bonferroni post-hoc test. Survival was analyzed by Kaplan-Meier method and the Mantel-Cox Log-Rank test. Disease-free survival time after surgery was calculated by Kaplan-Meier analysis, and was compared among groups by log-rank test using SPSS Statistics 22.0 software (IBM).

Results

IL17RB positivity in tumor tissues is a poor prognostic factor in breast cancer

We immunohistochemically analyzed tumor tissues obtained from stage I-III breast cancer patients (n = 115) for IL17RB expression. IL17RB expression was observed in 31% of the patients, and the positivity (Level 1 + 2) was significantly associated with shorter diseases-free survival of the patients (P = 0.0298; **Figure 1**), albeit no significant associations with OS (P = 0.3238) and other clinicopathological data (**Table 1**). This suggests that IL17RB positivity in tumor tissues is a significant poor prognostic factor in breast cancer as reported elsewhere [7, 8].

IL17RB transduction confers cancer stem-like properties to murine mammary cancer 4T1 cells

To elucidate the mechanisms underlying the poor prognosis of patients with IL17RB$^+$ breast cancer, we established IL17RB transfectants (TR) and a mock transfectant (mock) as a control using murine mammary tumor IL17RB^{low} 4T1 cells. The TR cells formed sphere colonies even in the normal culture condition (**Figure 2A**), suggesting resistance to anoikis, which is a programmed cell death occurred upon cell detachment [14]. In the sphere colony formation assay, the colony size was much larger, and the number of colonies was significantly higher

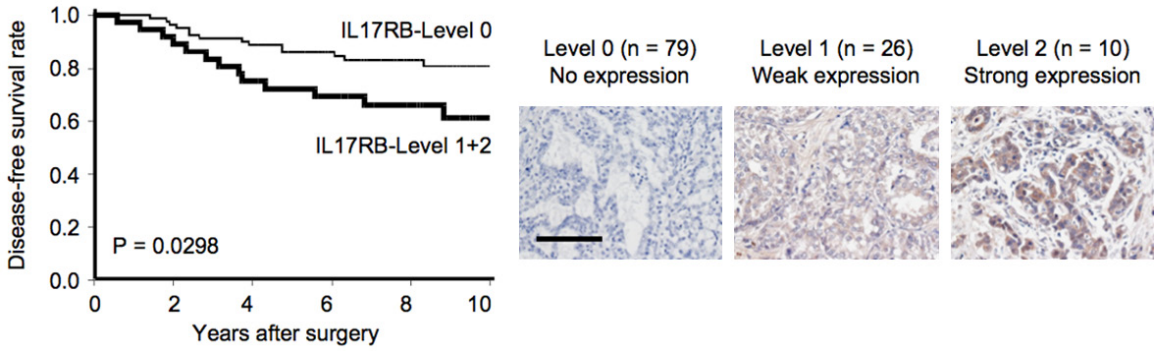

Figure 1. IL17RB positivity in tumor tissues is a poor prognostic factor in breast cancer. Tumor tissues obtained from stage I-III breast cancer patients (n = 115) were immunohistochemically analyzed for IL17RB expression, and the expression patterns were classified into 3 levels: Level 0, no expression; Level 1, weak expression; and Level 2, strong expression. Diseases-free survival of the patients was statistically compared between two groups divided by the positivity (Level 0 versus Level 1+2).

Table 1. Patient characteristics categorized by IL17RB expression levels in tumors

Characteristics	No. of patients (%)		
	Level 2 (n = 10)	Level 1 (n = 26)	Level 0 (n = 79)
Age (Median, range)	(57, 31-38)	(46, 34-80)	(55, 33-76)
Younger (< 60), n = 74	6 (8%)	19 (26%)	49 (66%)
Older (≥ 60), n = 41	4 (10%)	7 (17%)	30 (73%)
Sex			
Male, n = 0	0 (0%)	0 (0%)	0 (0%)
Female, n = 115	10 (9%)	26 (23%)	79 (69%)
T stage			
I, n = 61	5 (8%)	10 (16%)	46 (75%)
II, n = 49	4 (8%)	15 (30%)	30 (61%)
III, n = 5	1 (20%)	1 (20%)	3 (60%)
N stages			
0, n = 70	5 (7%)	12 (17%)	53 (76%)
I, n = 30	2 (7%)	8 (27%)	20 (67%)
II, n = 10	1 (10%)	4 (40%)	5 (50%)
III, n = 5	2 (40%)	2 (40%)	1 (20%)
Histological grades			
I, n = 40	3 (8%)	9 (33%)	28 (10%)
II, n = 52	6 (10%)	11 (36%)	35 (18%)
III, n = 22	1 (14%)	6 (23%)	15 (0%)
Unknown, n = 1	0 (0%)	0 (0%)	1 (0%)
Subtypes			
HR-HER2-, n = 6	0 (0%)	2 (33%)	4 (67%)
HR-HER2+, n = 5	1 (20%)	0 (0%)	4 (80%)
HR+HER2-, n = 91	8 (9%)	21 (23%)	62 (68%)
HR+HER2+, n = 13	1 (8%)	3 (23%)	9 (69%)

Level 0, no stained cells (no staining); Level 1, 1-50% (weak staining); and Level 2, 50-100% (strong staining).

as compared to those of the mock control ($P < 0.002$; **Figure 2B**). The invasive ability of the TR cells was significantly higher than that of the mock ($P < 0.001$), although proliferative ability was significantly lower ($P < 0.001$; **Figure 2B**). IL17RB transduction simultaneously upregulated its counterpart receptor IL17RA (**Figure 2A**) and cancer stem-related transcriptional factors (*snail*, twist, *aurka*, and *bcl2*) in the TR cells (**Figure 2C**). The TR cells were highly resistant to the CDKI treatments in the in vitro ($P < 0.001$ versus mock; **Figure 2D**) and in vivo settings ($P = 0.001$ versus TR-PBS; **Figure 2E**), although the treatments were significantly effective in the mock cases. These results suggest that IL17RB plays a key role in breast cancer stemness, and contributes to CDKI resistance.

IL17RB+ tumor cells systemically expand IL25+ macrophages in the implanted mice

To examine the immunological mechanisms induced by the IL17RB+ breast cancer, we implanted the tumor cells into mice, and analyzed immune cells in tumor tissues and spleen of the mice by flow cytometry. In vivo TR growth was also significantly slower than the mock growth ($P < 0.001$; **Figure 3A**), but F4/80+ macrophages (Møs) and

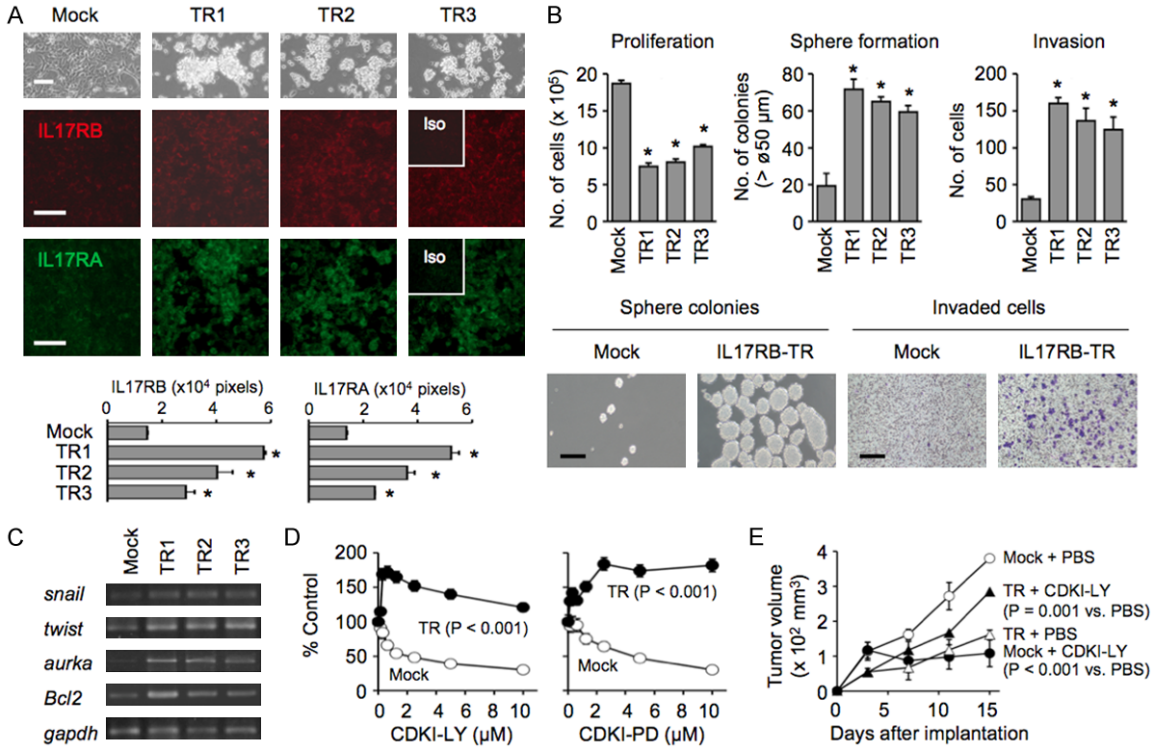

Figure 2. IL17RB transduction confers cancer stem-like properties to murine mammary cancer 4T1 cells. A. IL17RB transduction simultaneously upregulates IL17RA expression, and confers anoikis resistance. Murine mammary cancer 4T1 cells were transfected with a plasmid vector encoding murine *il17rb* (TR1, TR2, and TR3) or the empty vector as mock control (mock). The immunofluorescence intensity was measured as pixel counts at 400× magnification (3 fields per slide × 2 slides/clone, n = 6). Scale = 100 μm. B. IL17RB transduction confers high self-renewal and invasive on tumor cells (n = 3). Photos show the appearance of sphere colony formation and invaded cells (scale = 100 μm). C. IL17RB transduction simultaneously upregulates gene expression related to cancer stemness. RT-PCR was conducted to analyze gene expression in the tumor cells. D. The IL17RB$^+$ tumor cells are resistant to cyclin-dependent kinase 4/6 inhibitors. The TR cells (closed circles) or mock cells (open circles) were cultured with abemaciclib/LY2835219 (CDKI-LY) or palbociclib/PD0332991 (CDKI-PD) for 2 days, and the cell proliferation was assessed by WST1 assay (n = 3). Graphs were depicted as the percentage of the control without agents (100%). E. CDKI therapy rather promotes IL17RB$^+$ tumor growth in the implanted mice. BALB/c mice were subcutaneously (s.c.) implanted with tumor cells (5 × 10^5), and were orally administered with CDKI-LY (5 mg/kg) or PBS as a control daily on days 3-7 after tumor implantation (n = 5). Mock + PBS, open circles. Mock + CDKI-LY, closed circles. TR + PBS, open triangles. TR + CDKI-LY, closed triangles. All graphs show means ± SDs. *P < 0.01, **P < 0.05 versus mock control. Representative data of an experiment out of three independent experiments with consistent results.

potentially exhausted CD4$^+$/CD8$^+$ T cells and CD3$^-$DX5$^+$ NK cells significantly increased in the TR tumors (P < 0.01 versus mock; **Figure 3B**). Interestingly, only F4/80$^+$ Møs significantly increased in spleen of the TR tumor-implanted mice (P < 0.003 versus mock), although other cell populations, such as T cells and NK cells, significantly decreased (**Figure 3C**). Cytotoxic activities of the splenic CTLs (P = 0.002) and NK cells (P = 0.002) were extremely reduced as compared to those of the mock-implanted mice (**Figure 3D**). Considering the ligands for IL17RB, we tested the Møs for IL17B and IL17E/IL25 by immunostaining and ELISA. The Møs obtained from TR-implanted mice (designated TR-Møs) highly expressed IL25, but not IL17B, albeit almost no expression in the Møs obtained from mock-implanted mice (designated mock-Møs; **Figure 3E**). These implied that the Mø-derived IL25 might be involved in the CTL impairment in the IL17RB$^+$ tumor-implanted mice. Indeed, TR-Mø addition to the regular CTL induction system significantly inhibited induction of potent CTLs (P < 0.001 versus mock-Møs), but anti-IL25 mAb addition partly but significantly rescued from the TR-Mø-induced hindrance (P < 0.001; **Figure 3F**). These suggest that IL17RB$^+$ tumor cells impede induction of anti-

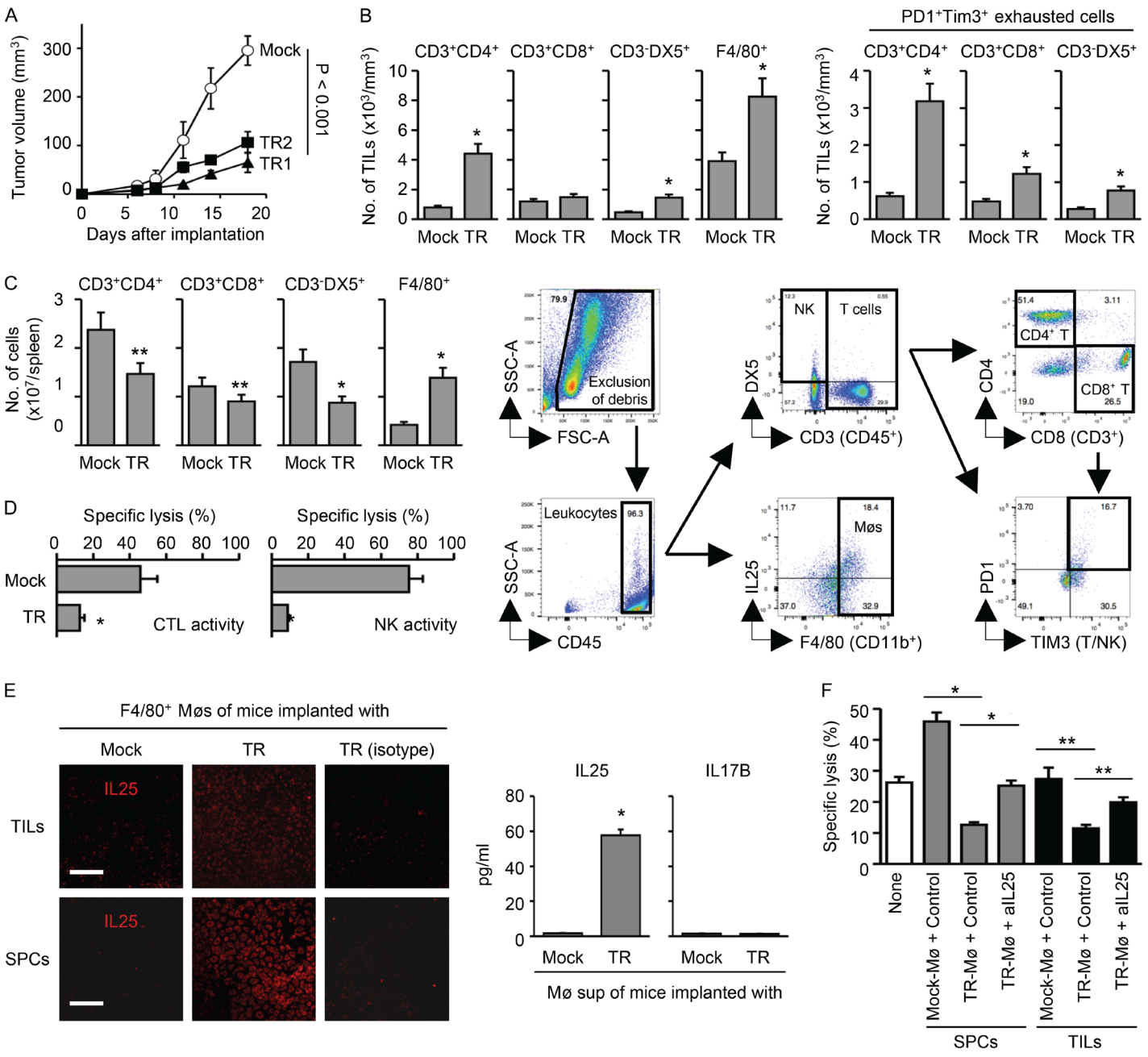
A
Tumor volume (mm3)
Mock
TR2
TR1
P < 0.001
Days after implantation
B
CD3+CD4+
CD3+CD8+
CD3-DX5+
F4/80+
No. of TILs (x10³/mm³)
Mock TR
PD1+Tim3+ exhausted cells
C
No. of cells (x10⁷/spleen)
D
Specific lysis (%)
Mock
TR
CTL activity
NK activity
Exclusion of debris
SSC-A
FSC-A
NK
T cells
DX5
CD3 (CD45+)
CD4+ T
CD8+ T
CD4
CD8 (CD3+)
Leukocytes
CD45
Møs
IL25
F4/80 (CD11b+)
PD1
TIM3 (T/NK)
E
F4/80+ Møs of mice implanted with
Mock
TR
TR (isotype)
TILs
SPCs
IL25
IL17B
pg/ml
Mø sup of mice implanted with
F
Specific lysis (%)
None
Mock-Mø + Control
TR-Mø + Control
TR-Mø + aIL25
SPCs
TILs

Figure 3. IL17RB+ tumor cells systemically expand IL25+ macrophages in the implanted mice. A. IL17RB+ tumor growth is retarded after implantation in mice. The TR (closed triangles and squares) or mock cells (open circles) were s.c. implanted in mice (5×10^5, n = 5). B. F4/80+ macrophages (Møs) and possibly exhausted CD3+PD1+Tim3+ T cells increase in the TR tumors (day 15 after implantation, n = 3). C. F4/80+ Møs also systemically increase in spleen of the TR-implanted mice (day 15; n = 3). D. Cytotoxic activities of anti-tumor effector cells are extremely reduced in the TR-implanted mice. CD8+ T cells were isolated from spleen cells (SPCs) stimulated with a tumor antigen AH1 peptide (1 μg/ml) for 6 days, and the sorted CD8+ T cells as CTLs were co-cultured with 4T1 cells as a target at ET ratio = 40:1 for 4 hours (n = 3). Splenic DX5+ NK cells were also co-cultured with Yac1 cells as a target at ET ratio = 20:1 for 4 hours (n = 3). E. The IL17RB+ tumor-induced Møs highly produce IL25. F4/80+ Møs were isolated from tumor-infiltrating cells (TILs) and SPCs of mice on day 15 after implantation with mock tumors (mock-Mø) or TR tumors (TR-Mø), and the adherent Møs after 2-hour-culture were stained with anti-IL25 mAb or the isotype control (n = 10, pooled). Scale = 100 μm. The 6-day-cultured splenic Mø supernatant was also tested for IL25 or IL17B by ELISA (n = 3). F. The IL17RB+ tumor-induced Møs suppress CTL induction partly by the secreted IL25. The sorted F4/80+ Møs were cocultured with the AH1-prestimulated CD8+ T cells in the presence of the AH1 peptide (10 μg/ml), IL2 (100 IU/ml), and anti-IL25 mAb or mIgG as a control (10 μg/ml) for 6 days, and the sorted CD8+ T cells were tested for cytotoxic activity (ET ratio = 20:1; n = 3). All graphs show means ± SDs. *P < 0.01, **P < 0.05 versus mock control. Representative data of an experiment out of three independent experiments with consistent results.

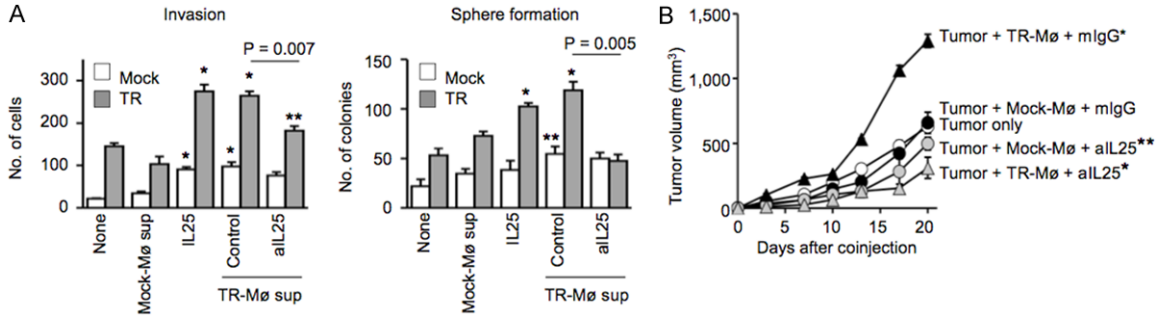

Figure 4. The IL17RB+ tumor-induced Møs intensify tumor functions. A. The TR-Møs enhance tumor invasive and self-renewal abilities partly utilizing the secreted IL25. Tumor cells were stimulated with IL25 (10 ng/ml) or the 6-day-cultured F4/80+ Mø supernatants (6 days) in the presence of anti-IL25 mAb or mIgG as a control (10 μg/ml) for 3 days before assays (n = 3). B. The TR-Møs promote in vivo tumor progression utilizing the secreted IL25. 4T1 cells were s.c. coinjected (1:1) with splenic Møs in mice, and the subcutaneous tumors were injected with anti-IL25 mAb or mIgG as a control (100 μg) on days 3 and 10 after coinjection (n = 5). Open circles, tumor only. Closed circles, tumor + mock-Møs + mIgG. Gray circles, tumor + mock-Møs + anti-IL25 mAb. Closed triangles, tumor + TR-Møs + mIgG. Gray triangles, tumor + TR-Møs + anti-IL25 mAb. All graphs show means ± SDs. *P < 0.01, **P < 0.05 versus mock. Representative data of an experiment out of three independent experiments with consistent results.

tumor immunity partly via expansion of the IL25+ Møs in the host.

The IL17RB+ tumor-induced Møs intensify tumor functions

To examine the IL25+ Mø effect on tumors, the Mø supernatant was added to the tumor culture. We used splenic Møs for further experiments, since the number of tumoral Møs was too small to conduct many different assays. Addition of the TR-Mø supernatant significantly enhanced invasive and self-renewal abilities of tumor cells (P < 0.01), particularly of TR cells, and the promotive effects were significantly suppressed by addition of anti-IL25 mAb (P < 0.01; **Figure 4A**). When parental 4T1 cells were coinjected (1:1) with the TR-Møs in mice, tumor growth was significantly promoted (P = 0.019 versus tumor only), but intratumoral injection with anti-IL25 mAb (to directly modulate the tumor environment) greatly suppressed the adverse tumor progression (P < 0.001 versus mIgG; **Figure 4B**). These suggest that the IL25+ Møs directly facilitate tumor progression utilizing the secreted IL25, but blocking IL25 is effective in abrogating the unfavorable effects.

Blocking IL25 improves anti-tumor efficacy induced by the CDK4/6 inhibitory therapy in mouse breast cancer models

Interestingly, the IL25+ Møs further increased in both tumors and spleen of the TR-implanted mice after the CDKI therapy (**Figure 5A**), and the cytotoxic activities of the splenic CTLs and NK cells were not improved in the mice (**Figure 5B**). However, anti-IL25 therapy significantly

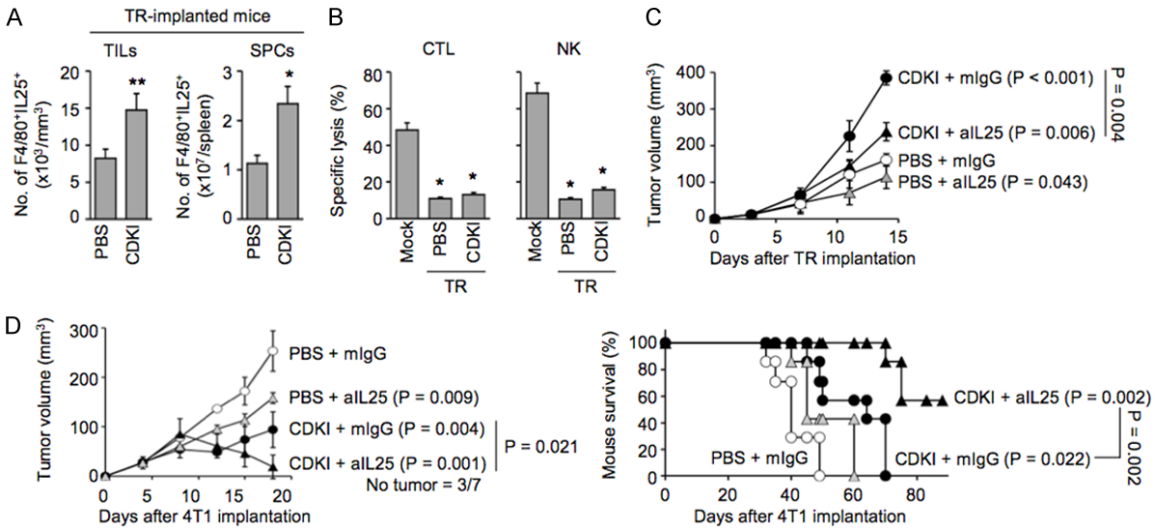

Figure 5. Blocking IL25 improves anti-tumor efficacy induced by the CDK4/6 inhibitory therapy in mouse breast cancer models. A. IL25+F4/80+ Møs and possibly exhausted CD3+CD8+PD1+Tim3+ T cells further increase in the TR-implanted mice after the CDKI therapy (day 15; n = 5). B. Cytotoxic activities of the splenic CTLs (ET ratio = 50:1; n = 3) and NK cells (ET ratio = 25:1; n = 3) remain reduced in the TR-implanted mice after the CDKI therapy. C. Anti-IL25 therapy suppresses the CDKI-induced TR tumor progression (n = 5). Mice were s.c. implanted with the TR cells (5×10^5), and received treatments: oral administration with CDKI-LY (5 mg/kg) or PBS as a control daily on days 3-7 after tumor implantation, and/or i.p. injection with anti-IL25 mAb or mIgG as a control (10 mg/kg) on days 3 and 7. Open circles, PBS + mIgG. Closed circles, CDKI-LY + mIgG. Gray triangles, PBS + anti-IL25 mAb. Closed triangles, CDKI-LY + anti-IL25 mAb. D. Anti-IL25 therapy synergizes with CDKI therapy in 4T1 tumor models (n = 7). Mice were s.c. implanted with parental 4T1 cells (but not TR, 5×10^5), and received treatments: oral administration with CDKI-LY (5 mg/kg) or PBS as a control daily on days 4-8 after tumor implantation, and/or i.p. injection with anti-IL25 mAb or mIgG as a control (10 mg/kg) on days 4 and 8. Open circles, PBS + mIgG. Closed circles, CDKI-LY + mIgG. Gray triangles, PBS + anti-IL25 mAb. Closed triangles, CDKI-LY + anti-IL25 mAb. All graphs show means ± SDs. *P < 0.01, **P < 0.05 versus mock. Representative data of an experiment out of three independent experiments with consistent results.

suppressed the CDKI-induced TR progression (P = 0.004 versus mIgG; **Figure 5C**). The combination regimen with CDKI and anti-IL25 mAb was significantly effective in regular 4T1 tumor models, and subcutaneous tumors finally disappeared in 43% (3/7) of the treated mice (**Figure 5D**). Survival of the treated mice was significantly prolonged as compared to that of the mice receiving CDKI only, indicating a synergistic effect (P = 0.002; **Figure 5D**). The surviving mice on day 100 completely rejected rechallenged 4T1 tumors, indicating immunological memory induction in the treated mice. These suggest that anti-IL25 therapy is useful to optimize the CDKI-induced efficacy in the treatment of breast cancer.

Significance of the IL17RB-IL25 axis in human breast cancer system

To validate these findings in the human system, we established IL17RB transfectants and the mock control using human breast cancer IL17RB- MCF7 cells. The MCF7-TR cells showed significantly higher self-renewal and invasive abilities (P < 0.001; **Figure 6A**), and were resistant to CDKI treatment (P < 0.001; **Figure 6B**). In vitro proliferation and in vivo growth of the MCF-TR were significantly retarded, and IL25+ Møs significantly increased in the tumors (P < 0.001 versus mock; **Figure 6C**). Splenic F4/80+ Møs obtained from the TR-implanted mice (day 30) highly produced IL25 (P < 0.0001 versus mock-Møs; **Figure 6D**). The combination regimen with CDKI and anti-IL25 mAb significantly suppressed tumor growth in the MCF7-implanted xenograft tumor models (P = 0.016 versus CDKI only; **Figure 6E**). These results were consistent with the results observed in the mouse system.

Collectively, IL17RB+ tumor-induced IL25+ Mø is a key booster of the IL17RB+ tumor progression, and thus targeting the IL17RB-IL25 axis may be a promising strategy for improving the clinical outcomes in the treatment of breast

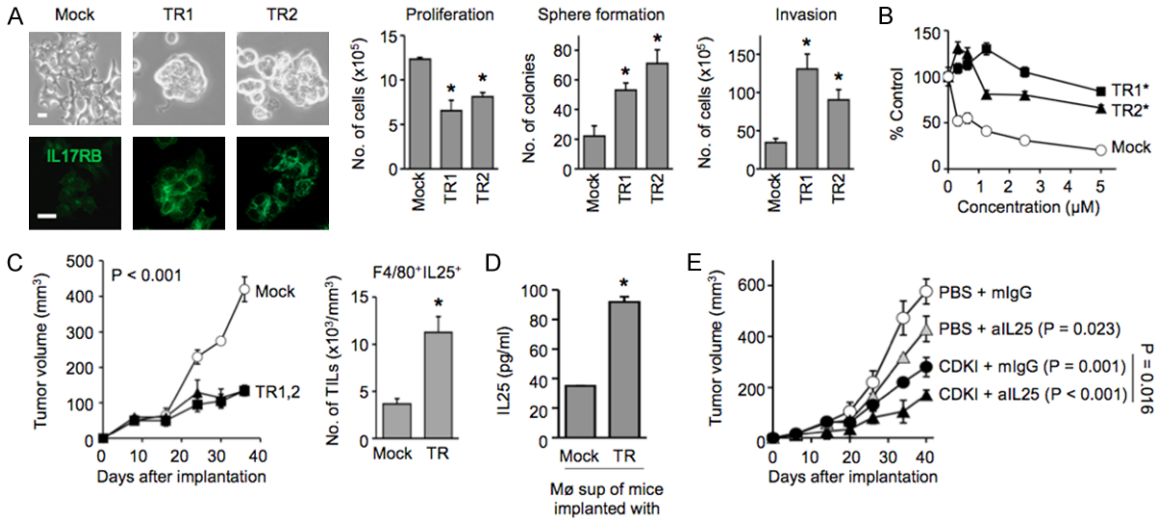

Figure 6. Significance of the IL17RB-IL25 axis in human breast cancer system. A. IL17RB transduction confers high self-renewal and invasive properties on human breast cancer (n = 3). Human breast cancer MCF7 cells were transfected with a plasmid vector encoding human *il17rb* (2 clones: TR1 and TR2) or the empty vector as mock control (mock). Photos show IL17RB expression and anoikis-resistant appearance (scale = 100 μm). B. The IL17RB⁺ tumor cells are resistant to CDKI treatment. The TR cells (closed triangles and squares) or mock cells (open circles) were cultured with CDKI-LY for 2 days, and the cell proliferation was assessed by WST1 assay (n = 3). Graphs were depicted as the percentage of the control without agents (100%). C. IL17RB⁺ tumor growth is retarded after implantation in mice. The TR (closed triangles and squares) or mock cells (open circles) were s.c. implanted in immunodeficient nude mice (1×10^6, n = 5). D. The IL17RB⁺ tumor-expanded Møs highly produce IL25. F4/80⁺ Møs were isolated from SPCs of the tumor-implanted mice (day 30), and the 6-day-cultured Mø supernatants were tested for IL25 by ELISA (n = 3). E. Combination therapy with CDKI and anti-IL25 mAb significantly suppresses tumor progression in the xenograft models (n = 5). Nude mice were s.c. implanted with parental MCF7 cells (1×10^6), and received two cycles of the treatments: oral administration with CDKI-LY (5 mg/kg) or PBS as a control daily on days 5-9 and days 16-20 after tumor implantation, and/or i.p. injection with anti-IL25 mAb or mIgG as a control (10 mg/kg) on days 5, 9, 16 and 20. Open circles, PBS + mIgG. Closed circles, CDKI-LY + mIgG. Gray triangles, PBS + anti-IL25 mAb. Closed triangles, CDKI-LY + anti-IL25 mAb. All graphs show means ± SDs. *P < 0.01 versus mock. Representative data of an experiment out of three independent experiments with consistent results.

cancer patients, particularly with IL17RB⁺ tumors. Blocking IL25 may greatly contribute to the CDKI therapy that the therapeutic efficacy is still low in the clinical settings despite numerous trials.

Discussion

This study revealed tumor biological and immunological mechanisms underlying the poor prognosis of hosts with IL17RB⁺ breast cancer. IL17RB overexpression confers cancer stemness, including high resistance to anoikis and CDKIs, and high invasive and self-renewal abilities accompanied by upregulation of cancer stem-governing transcriptional factors, to breast cancer cells. The IL17RB⁺ tumor cells proliferate much slowly in a quiescent status, but show over-proliferation in response to CDKI treatment. Such abnormal cell division, including both dormant/quiescent slow-cycling hypoproliferative and hyperproliferative properties, is representative of cancer stemness, and hypoproliferative tumor cells are known to convert to a hyperproliferative type upon stimulation due to its high plasticity [15, 16]. IL17RA expression is also upregulated in the IL17RB⁺ tumor cells. IL17RA gene is ubiquitously expressed in most cells, and its protein expression is promptly upregulated by stimulation with proinflammatory cytokines, albeit in immune cell cases [17]. Multiple stimulations with simultaneously upregulated cytokines might have induced IL17RA protein expression in an autocrine manner, although further studies are needed. The IL17RB⁺ tumor cells facilitate own progression also by local and systemic expansion of IL25⁺ Møs, which enhance tumor functions and suppress induction of anti-tumor immunity utilizing the secreted IL25. Blocking IL25, however, successfully breaks the CDKI resistance of the IL17RB⁺ tumors. These sug-

gest that the IL25+ Mø is a prominent ally to accelerate the vicious cycle for further progression of the IL17RB+ tumors. Targeting the IL17RB-IL25 axis may be a promising strategy for improving clinical outcomes in the treatment of breast cancer patients, particularly with IL17RB+ refractory tumors.

IL17B has always been the center in the mechanisms underlying the IL17RB+ refractory breast cancer, and targeting the IL17RB-IL17B axis has attracted attention in the treatment of breast cancer [7, 8]. Surely, IL17B has been reported to play a key roles in tumorigenesis [18] and chemoresistance [19] of IL17RB+ breast cancer. However, in our study, IL25, but not IL17B, was absolutely required for the IL17RB+ breast cancer progression. IL25 is known to enhance self-renewal and metastatic abilities directly and indirectly via inducing polarization of M2-type Møs and Th2 [20], and anti-IL25 therapeutic efficacy on tumor metastasis has been shown in mouse breast cancer models [21]. However, functional roles of IL25 are still controversial due to the inconsistent results. For example, a paper showed that IL25 secreted from nonmalignant mammary epithelial cells induces apoptosis in breast cancer cells, and suppresses in vitro colony formation and in vivo tumor growth [22]. The same group also reported that IL25 secreted from tumor-associated fibroblasts induces apoptosis in breast cancer cells, and suppresses tumor metastasis [23]. In our study, however, IL25 stimulation (10 ng/ml for 3 days) significantly enhanced tumor functions rather than inducing cell death. In their experiments, a much higher dose (200-500 ng/ml) was used to stimulate tumor cells in the in vitro culture for much longer time (10 days). In the in vivo setting, a high dose of IL25 (200 ng × 3 injection/week × 3 weeks) was injected into mouse tumor models for a long time. According to the data shown in the ProteinAtlas database (https://www.proteinatlas.org), IL25 concentration is 3.1-90 pg/ml in blood of healthy donors, and allergic asthma and rheumatoid arthritis patients, albeit not including cancer patients. Even if considering the half-life in the in vivo setting, the doses used in their experiments seem to be quite higher than physiological status, and thus might have produced inconsistency in the results.

Our study showed that the Mø-derived IL25 was a key effector molecule in the IL17RB+ tumor progression mechanisms. The Jiang et al. reported metastatic activity of IL25 that is derived from not only Møs but also CD4+ T cells in the tumor microenvironment using another mouse breast cancer model, which is genetically engineered mammary specific polyomavirus middle T antigen overexpressing tumor models (MMTV-PyMT) [21]. In the study, anti-IL25 therapy showed anti-tumor effect on lung metastasis, but not primary tumor growth and mouse survival. However, they did not show IL25+ cells in the metastatic lung tissues. Also, they showed numerous IL25+ Møs, but very few IL25+CD4+ cells, by immunostaining, suggesting the major source of IL25 is Møs. They showed IL25 expression by PCR and immunostaining, but not by ELISA to detect actual release of IL25. In our study, we showed local and systemic increase of Møs that actually release IL25, and anti-IL25 therapeutic efficacy on tumor growth and mouse survival. Such discrepancy might have arisen from the differences in the tumor models and techniques.

The IL25+ Møs were further expanded in the mice with IL17RB+ tumors after CDKI therapy, and the IL17RB+ tumor growth was adversely promoted in the mice. However, blocking IL25 interfered the adverse events. The combination regimen with anti-IL25 mAb and CDKI provided more than 40% of complete remission in the regular 4T1 tumor models, and was also significantly effective even in xenograft tumor models with no T-cell immunity. CDKI therapeutic efficacy is still low in breast cancer, despite numerous clinical trials in combination with many different types of treatments [5, 6]. Anti-IL25 therapy may be a better treatment to successfully elicit the CDKI-therapeutic efficacy in breast cancer patients, particularly with IL17RB+ tumors. Unfortunately, many side effects, such as neutropenia, leukopenia, fatigue and nausea, have been reported in CDKI therapy, and the management is important in the clinical settings [24]. About the side effects of anti-IL25 therapy, we speculate as follows: IL-25 is known to function as a skin barrier cytokine to protect from tissue damage leading to inflammatory diseases, such as atopic dermatitis, psoriasis, and asthma [25]. In addition, IL25 treatment is known to protect from obesity and related metabolic disorders in the mice

fed with a high-fat diet through beige fat formation in white adipose tissue [26]. Therefore, it is inferred that blocking IL25 may delay wound healing in injured patients, and may cause obesity and related metabolic disorders as side effects in the clinical settings, although none of them were observed at least in our therapeutic experiments using mouse tumor models.

How IL17RB$^+$ tumor cells induce IL25$^+$ Møs remains to be clarified. We speculate involvement of some molecules, such as IL33 [27] and GDF15 [28] that we previously identified as key effector molecules released from AURKA$^+$ polyploid tumors, which are resistant to small molecule inhibitors, including CDKIs. Polyploid tumors show adverse progression in the treatment just like IL17RB$^+$ tumors. Cancer polyploidization is a principal program in cancer stemness to massively increase intratumoral heterogeneity and complexity by generating numerous progeny cells from giant cells in response to treatment stress [29]. Identification of the IL25$^+$ Mø inducer derived from the IL17RB$^+$ tumors may greatly contribute to the optimization of the combination regimen that we established in this study.

Our study demonstrated that the IL17RB positivity in tumors and the IL25$^+$ Møs may be possibly good biomarkers to predict possible responses to CDKI therapy in breast cancer. IL25 increase in peripheral blood has been reported in breast cancer patients [30]. In such patients, tumor cells may highly express IL17RB, and IL25$^+$ Møs may be expanded for supplying IL25 as a source. The serum IL25 seems to be a more easy-to-test biomarker. Further study using more clinical samples, including tumor tissues and peripheral blood obtained from CDKI-treated patients, is needed for clarification of the clinical relevancy of the relationships among IL17RB$^+$ tumors, IL25$^+$ Møs, and CDKI resistance.

In conclusion, targeting the IL17RB-IL25 axis may be a promising diagnostic and therapeutic strategy for improving the clinical outcomes in the treatment of breast cancer patients, particularly with IL17RB$^+$ tumors. We hope that our findings will facilitate the practical implementation in the clinical settings.

Acknowledgements

This study was financially supported by the Japan Agency for Medical Research and Development P-CREATE, Tokyo, Japan (106209 to C.K.-S.), and Grants-in-Aid for Scientific Research KAKENHI (19K18073 to Y.O.). The authors thank Ms. Kana Uegaki for the technical support throughout this study.

Disclosure of conflicts of interest

None.

Address correspondence to: Chie Kudo-Saito, Department of Immune Medicine, National Cancer Center Research Institute, Tokyo 104-0045, Japan. E-mail: ckudo@ncc.go.jp

References

[1] Siegel RL, Miller KD and Jemal A. Cancer statistics, 2020. CA Cancer J Clin 2020; 70: 7-30.
[2] Loibl S, Poortmans P, Morrow M, Denkert C and Curigliano G. Breast cancer. Lancet 2021; 397: 1750-1769.
[3] Goel S, Bergholz JS and Zhao JJ. Targeting CDK4 and CDK6 in cancer. Nat Rev Cancer 2022; 22: 356-372.
[4] Pandey K, An HJ, Kim SK, Lee SA, Kim S, Lim SM, Kim GM, Sohn J and Moon YW. Molecular mechanisms of resistance to CDK4/6 inhibitors in breast cancer: a review. Int J Cancer 2019; 145: 1179-1188.
[5] Papadimitriou MC, Pazaiti A, Iliakopoulos K, Markouli M, Michalaki V and Papadimitriou CA. Resistance to CDK4/6 inhibition: mechanisms and strategies to overcome a therapeutic problem in the treatment of hormone receptor-positive metastatic breast cancer. Biochim Biophys Acta Mol Cell Res 2022; 1869: 119346.
[6] Xi J and Ma CX. Sequencing endocrine therapy for metastatic breast cancer: what do we do after disease progression on a CDK4/6 inhibitor? Curr Oncol Rep 2020; 22: 57.
[7] Alinejad V, Dolati S, Motallebnezhad M and Yousefi M. The role of IL17B-IL17RB signaling pathway in breast cancer. Biomed Pharmacother 2017; 88: 795-803.
[8] Bastid J, Dejou C, Docquier A and Bonnefoy N. The emerging role of the IL-17B/IL-17RB pathway in cancer. Front Immunol 2020; 11: 718.
[9] Kudo-Saito C, Ozaki Y, Imazeki H, Hayashi H, Masuda J, Ozawa H and Ogiwara Y. Targeting oncoimmune drivers of cancer metastasis. Cancers (Basel) 2021; 13: 554.
[10] Kudo-Saito C, Fuwa T, Murakami K and Kawakami Y. Targeting FSTL1 prevents tumor bone metastasis and consequent immune dysfunction. Cancer Res 2013; 73: 6185-6193.
[11] Kudo-Saito C, Shirako H, Takeuchi T and Kawakami Y. Cancer metastasis is accelerated through immunosuppression during Snail-

induced EMT of cancer cells. Cancer Cell 2009; 15: 195-206.
[12] Ogiwara Y, Nakagawa M, Nakatani F, Uemura Y, Zhang R and Kudo-Saito C. Blocking FSTL1 boosts NK immunity in treatment of osteosarcoma. Cancer Lett 2022; 537: 215690.
[13] Scrimieri F, Askew D, Corn DJ, Eid S, Bobanga ID, Bjelac JA, Tsao ML, Allen F, Othman YS, Wang SC and Huang AY. Murine leukemia virus envelope gp70 is a shared biomarker for the high-sensitivity quantification of murine tumor burden. Oncoimmunology 2013; 2: e26889.
[14] Khan SU, Fatima K and Malik F. Understanding the cell survival mechanism of anoikis-resistant cancer cells during different steps of metastasis. Clin Exp Metastasis 2022; 39: 715-726.
[15] Talukdar S, Bhoopathi P, Emdad L, Das S, Sarkar D and Fisher PB. Dormancy and cancer stem cells: an enigma for cancer therapeutic targeting. Adv Cancer Res 2019; 141: 43-84.
[16] Greten FR and Grivennikov SI. Inflammation and cancer: triggers, mechanisms, and consequences. Immunity 2019; 51: 27-41.
[17] Gaffen SL. Structure and signalling in the IL-17 receptor family. Nat Rev Immunol 2009; 9: 556-567.
[18] Huang CK, Yang CY, Jeng YM, Chen CL, Wu HH, Chang YC, Ma C, Kuo WH, Chang KJ, Shew JY and Lee WH. Autocrine/paracrine mechanism of interleukin-17B receptor promotes breast tumorigenesis through NF-kappaB-mediated antiapoptotic pathway. Oncogene 2014; 33: 2968-2977.
[19] Laprevotte E, Cochaud S, du Manoir S, Lapierre M, Dejou C, Philippe M, Giustiniani J, Frewer KA, Sanders AJ, Jiang WG, Michaud HA, Colombo PE, Bensussan A, Alberici G, Bastid J, Eliaou JF and Bonnefoy N. The IL-17B-IL-17 receptor B pathway promotes resistance to paclitaxel in breast tumors through activation of the ERK1/2 pathway. Oncotarget 2017; 8: 113360-113372.
[20] Gowhari Shabgah A, Amir A, Gardanova ZR, Olegovna Zekiy A, Thangavelu L, Ebrahimi Nik M, Ahmadi M and Gholizadeh Navashenaq J. Interleukin-25: new perspective and state-of-the-art in cancer prognosis and treatment approaches. Cancer Med 2021; 10: 5191-5202.
[21] Jiang Z, Chen J, Du X, Cheng H, Wang X and Dong C. IL-25 blockade inhibits metastasis in breast cancer. Protein Cell 2017; 8: 191-201.
[22] Furuta S, Jeng YM, Zhou L, Huang L, Kuhn I, Bissell MJ and Lee WH. IL-25 causes apoptosis of IL-25R-expressing breast cancer cells without toxicity to nonmalignant cells. Sci Transl Med 2011; 3: 78ra31.
[23] Yin SY, Jian FY, Chen YH, Chien SC, Hsieh MC, Hsiao PW, Lee WH, Kuo YH and Yang NS. Induction of IL-25 secretion from tumour-associated fibroblasts suppresses mammary tumour metastasis. Nat Commun 2016; 7: 11311.
[24] Thill M and Schmidt M. Management of adverse events during cyclin-dependent kinase 4/6 (CDK4/6) inhibitor-based treatment in breast cancer. Ther Adv Med Oncol 2018; 10: 1758835918793326.
[25] Borowczyk J, Shutova M, Brembilla NC and Boehncke WH. IL-25 (IL-17E) in epithelial immunology and pathophysiology. J Allergy Clin Immunol 2021; 148: 40-52.
[26] Li L, Ma L, Zhao Z, Luo S, Gong B, Li J, Feng J, Zhang H, Qi W, Zhou T, Yang X, Gao G and Yang Z. IL-25-induced shifts in macrophage polarization promote development of beige fat and improve metabolic homeostasis in mice. PLoS Biol 2021; 19: e3001348.
[27] Kudo-Saito C, Miyamoto T, Imazeki H, Shoji H, Aoki K and Boku N. IL33 is a key driver of treatment resistance of cancer. Cancer Res 2020; 80: 1981-1990.
[28] Ozawa H, Imazeki H, Ogiwara Y, Kawakubo H, Fukuda K, Kitagawa Y and Kudo-Saito C. Targeting AURKA in treatment of peritoneal tumor dissemination in gastrointestinal cancer. Transl Oncol 2022; 16: 101307.
[29] Zhou X, Zhou M, Zheng M, Tian S, Yang X, Ning Y, Li Y and Zhang S. Polyploid giant cancer cells and cancer progression. Front Cell Dev Biol 2022; 10: 1017588.
[30] Barati M, Sinaeian M, Shokrollahi Barough M, Pak F, Semnani V, Kokhaei P and Momtazi-Borojeni AA. Evaluation of interleukin 25 and interleukin 25 receptor expression in peripheral blood mononuclear cells of breast cancer patients and normal subjects. J Interferon Cytokine Res 2020; 40: 139-144.